Percolation analysis of a disordered spinor Bose gas

Sk Noor Nabi* and Saurabh Basu†
Department of Physics, Indian Institute of Technology Guwahati, Guwahati, Assam 781039, India
(Dated: April 21, 2015)

We study the effects of an on-site disorder potential in a gas of spinor (spin-1) ultracold atoms loaded in an optical lattice corresponding to both ferromagnetic and antiferromagnetic spin dependent interactions. Starting with a disordered spinor Bose-Hubbard model (SBHM) on a two dimensional square lattice, we observe the appearance of a Bose glass phase using the fraction of the lattice sites having finite superfluid order parameter and non integer local densities as an indicator. A precise distinction between three different types of phases namely, superfluid (SF), Mott insulator (MI) and Bose glass (BG) is done via a percolation analysis thereby demonstrating that a reliable enumeration of phases is possible at particular values of the parameters of the SBHM. Finally we present the phase diagram based on the above information for both antiferromagnetic and ferromagnetic interactions.

I. INTRODUCTION

The physical realization of spinor Bose gases is severely impeded by largely the instability of the internal atomic states. The excited states typically decay through spontaneous emission on time scales faster than that what is needed for the gas to equilibriate via collisions. However, owing to the huge technological success, dilute atomic gases with internal degrees of freedom have been realized. Optically trapped spin-1 ^{23}Na is among the first ones to be reported [1–6] . The progress has been rapid since then with the discovery of spin-1 [5, 7] and spin-2 manifold of ^{87}Rb [6], [8–10]. A flurry of activities have taken place since. It is beyond the scope of the present work to furnish the large volume of literature that exists on the progress of the study of spinor Bose gases. There is an extensive review by Stamper-Kurn and Ueda on the subject [11].

An interesting offshoot of the study of phase diagram of spinor Bose gases is to investigate the role of disorder present therein. Since inclusion of disorder in the context of an atomic gas loaded in an optical lattice is experimentally possible via speckle or periodic potentials [12–16], investigation of its influence on the phase diagram is a pertinent task.

Further, with the advent of techniques that can probe single atoms, the accessibility of the quantum world has been revolutionized, which can not be obtained by statistical sampling [17, 18]. This has made possible imaging of the insulating phase of the interacting atomic species of bosons on an optical lattice with a single atom and single site resolution. Among other things, such studies will furnish the population density of bosons (or the fluctuation therein) in different phases and their local tunneling dynamics in an optical lattice.

All of the above discussion would gain importance in the context of studying a system of spinor bosons in an inhomogeneous environment, that is in presence of disorder. The phase diagram of the spinor particles is in general richer owing to the different signs of the spin dependent interactions that render a polar or a ferromagnetic nature for the superfluid phase [4], [19, 20].

The '*theorem of inclusions*' [21] forbids a direct MI to a SF transition in presence of disorder. A BG phase always intervenes in between. Since a BG phase originates due to arbitrarily large, although rarely occurring clusters of one type of phase present amidst another, and as statistically rare events are difficult to sample, elegant methods such as stochastic mean-field theory [22–24], quantum Monte Carlo(QMC) etc [24], [25–27] were formulated and used to study the BG phase.

In this work we employ a single site mean field theory (SMFT) [28] which is very extensively and most commonly used tool and apply it for studying a Bose-Hubbard model (BHM) that recognizes the spin degree of freedom of the atomic gas (we call it SBHM). Corresponding to the disorder free scenario, the nature of phase transition in the antiferromagnetic and ferromagnetic cases are ascertained via the average order parameter and the local density fluctuation, that is the compressibility. The nature of the phase transition for the odd (occupation density 1, 3, 5..) and the even (occupation density 2, 4, 6..) Mott lobes are different for the polar fluid, while this is untrue for the ferromagnetic case (see discussion on antiferromagnetic and ferromagnetic cases in the next section).

In presence of disorder, we define a simple physical quantity, χ defined as the fraction of the sites with finite SF order parameter and non integer occupation density that will be used as indicators for the MI, BG or SF phases [29].

A percolation of the insulating sites is seen to occur with patches of the superfluid order surviving, thereby maintaining a zero macroscopic superfluid order, although compressible. The percolation scenario is robustly tested and a percolation threshold, implying the onset of a SF phase is obtained with the help of Hoshen-Kopelman(HK) algorithm [30]. Equipped with all of the above, we map out a phase diagram for the (F =1) spinor bosons in a two dimensional square (optical) lattice, where we specifically focus on the emergence and sustenance of the BG phase in both antiferromagnetic and ferromagnetic cases.

We organize our paper as follows. In the next section, we briefly review the mean field theory for the SBHM in the in-

* sk.noor@iitg.ernet.in
† saurabh@iitg.ernet.in

homogeneous case (in presence of disorder). In section III, we present the results for the average SF order parameter and the compressibility in both the antiferromagnetic and ferromagnetic cases. Further, we study the variation of χ in presence of disorder and the finite size scaling properties. We obtain the phase diagram based on this information and present it thereafter. Finally in section IV we outline our concluding remarks.

II. MODEL

The behavior of ultracold atoms loaded in an optical lattice with hyperfine spin F=1 can be well described by a SBHM [31] as,

$$\hat{H} = -t \sum_{<i,j>} \sum_{\sigma} (\hat{a}^{\dagger}_{i\sigma}\hat{a}_{i\sigma} + h.c) + \sum_i (\mu - \epsilon_i)\hat{n}_i + \sum_i \frac{U_0}{2}\hat{n}_i(\hat{n}_i - 1) + \frac{U_2}{2}(\mathbf{S}_i^2 - 2\hat{n}_i) \quad (1)$$

where t is the tunneling matrix, $\langle i,j\rangle$ are the nearest neighbour sites, μ is the chemical potential, U_0 describes the spin independent on-site interaction and U_2 is spin dependent interaction which arises due to the difference in scattering lengths a_0 and a_2 corresponding to S=0 and S=2 channels and U_0, U_2 are related to the scattering length by, $U_0 = (4\pi\hbar^2/M)((a_0+2a_2)/3)$ and U_2= $(4\pi\hbar^2/M)((a_2-a_0)/3)$. The spin dependent interaction, U_2 can have either positive or negative signs depending upon whether $a_2 > a_0$ or $a_2 < a_0$. Thus U_2 is antiferromagnetic (where the SF phase is polar) for $a_2 > a_0$ and ferromagnetic (where the SF phase being ferromagnetic) for $a_2 < a_0$. The total spin at site i is $\mathbf{S}_i = \hat{a}^{\dagger}_{i\sigma}\mathbf{F}_{\sigma\sigma'}\hat{a}_{i\sigma'}$ where $\mathbf{F}_{\sigma\sigma'}$ are the components of spin-1 matrices and σ=+1, 0, -1. The particle number operator, $\hat{n}_i = \sum_\sigma \hat{n}_{i\sigma}$, $\hat{n}_{i\sigma} = \hat{a}^{\dagger}_{i\sigma}\hat{a}_{i\sigma}$ where $\hat{a}^{\dagger}_{i\sigma}(\hat{a}_{i\sigma})$ is the boson creation (annihilation) operator at a site i. ϵ_i is the on-site disorder is introduced by the parameter i, which is randomly chosen from a box distribution extended over $[-\Delta, \Delta]$ where Δ is the strength of the disorder and an important parameter of our work. The components of the spin operator are given by,

$$\hat{S}_{iz} = \hat{a}^{\dagger}_{i+}\hat{a}_{i+} - \hat{a}^{\dagger}_{i-}\hat{a}_{i-} = \hat{n}_{i+} - \hat{n}_{i-}$$
$$\hat{S}_{ix} = \frac{1}{\sqrt{2}}(\hat{a}^{\dagger}_{i0}\hat{a}_{i+} + \hat{a}^{\dagger}_{i+}\hat{a}_{i0} + \hat{a}^{\dagger}_{i0}\hat{a}_{i-} + \hat{a}^{\dagger}_{i-}\hat{a}_{i0})$$
$$\hat{S}_{iy} = \frac{i}{\sqrt{2}}(\hat{a}^{\dagger}_{i0}\hat{a}_{i+} - \hat{a}^{\dagger}_{i+}\hat{a}_{i0} - \hat{a}^{\dagger}_{i0}\hat{a}_{i-} + \hat{a}^{\dagger}_{i-}\hat{a}_{i0})$$

$$S_i^2 = 2\hat{n}_{i+}\hat{n}_{i0} + 2\hat{n}_{i+}\hat{n}_{i0} + \hat{n}_{i+} + 2\hat{n}_{i0} + \hat{n}_{i-} + \hat{n}_{i+}^2 - 2\hat{n}_{i+}\hat{n}_{i-} + \hat{n}_{i-}^2 + 2\hat{a}^{\dagger}_{i+}\hat{a}^{\dagger}_{i-}\hat{a}^2_{i0} + 2\hat{a}_{i+}\hat{a}_{i-}\hat{a}^{\dagger 2}_{i0} \quad (2)$$

To solve Eq.(1), we shall employ SMFT that decouples the system Hamiltonian into sum of the single site Hamiltonians. The hopping part of the Hamiltonian can be decoupled as [19, 32],

$$\hat{a}^{\dagger}_{i\sigma}\hat{a}_{j\sigma} = \langle\hat{a}^{\dagger}_{i\sigma}\rangle\hat{a}_{j\sigma} + \hat{a}^{\dagger}_{i\sigma}\langle\hat{a}^{\dagger}_{j\sigma}\rangle - \langle\hat{a}^{\dagger}_{i\sigma}\rangle\langle\hat{a}^{\dagger}_{j\sigma}\rangle + \delta a^{\dagger}_{i\sigma}\delta a_{j\sigma} \quad (3)$$

where $\langle\hat{O}\rangle$ denotes the equilibrium value of an operator, $\hat{O}$ and $\delta a_{j\sigma} = \hat{a}_{j\sigma} - \langle\hat{a}_{j\sigma}\rangle$ denotes the fluctuations in $\hat{a}_{i\sigma}$. Now introducing the superfluid order parameter at site i as,

$$\psi_{i\sigma} \equiv \langle\hat{a}^{\dagger}_{i\sigma}\rangle = \sqrt{n_{s\sigma}}\xi^*_\sigma \equiv \langle\hat{a}_{i\sigma}\rangle = \sqrt{n_{s\sigma}}\xi_\sigma \quad (4)$$

where ψ_i=$\sqrt{\psi^2_{i\sigma}}$= $\sqrt{\psi^2_{i+} + \psi^2_{i0} + \psi^2_{i-}}$ and $n_{s\sigma}$ is the superfluid density and ξ_σ is a normalized spinor obeying $\sum_\sigma \xi^*_\sigma\xi_\sigma = 1$.

It is obvious that all spinors are related to each other by a gauge transformation, $e^{i\theta}$ and spin rotations, $u(\alpha,\beta,\tau) = e^{-iS_z\alpha}e^{-iS_y\beta}e^{-iS_z\tau}$ where (α,β,τ) are the Euler angles. The behavior of the SF order parameter is different in the antiferromagnetic and ferromagnetic regimes and are enumerated in the following [33–35].

(i) Antiferromagnetic case: when $U_2 > 0$, the spinor, ξ_σ is given by,

$$\xi = e^{i\theta}u\begin{pmatrix}0\\1\\0\end{pmatrix} = e^{i\theta}\begin{pmatrix}-\frac{1}{\sqrt{2}}e^{-i\alpha}sin\beta\\ cos\beta\\ \frac{1}{\sqrt{2}}e^{i\alpha}sin\beta\end{pmatrix} \quad (5)$$

If α=β=$\frac{\pi}{2}$ then ψ_+=ψ_- $\neq 0$, $\psi_0 = 0$ or α=$[0, 2\pi]$ and β=0 or π then ψ_+=ψ_-=0, $\psi_0 \neq 0$.

(ii) Ferromagnetic case: when $U_2 < 0$, ξ_σ is given by,

$$\xi = e^{i\theta}u\begin{pmatrix}1\\0\\0\end{pmatrix} = e^{i\theta}\begin{pmatrix}e^{-i\alpha}cos^2\beta/2\\ \sqrt{2}\ cos\beta/2\ \ sin\beta/2\\ e^{i\alpha}sin^2\beta/2\end{pmatrix} \quad (6)$$

If $\beta = \pi/2$ and $\alpha = 0$ then $\psi_+ = \psi_-$, $\psi_0 = \sqrt{2}\psi_+$.

Now neglecting the quadratic fluctuations and substituting the superfluid order parameter in Eq.(1), the SBHM can be written as a sum of single site Hamiltonians as,

$$H = \sum\nolimits_i H_i^{MF}$$

where

$$H_i^{MF} = -t\sum_\sigma(\phi^*_{i\sigma}\hat{a}_{i\sigma} + \phi_{i\sigma}\hat{a}^{\dagger}_{i\sigma}) + t\sum_\sigma\phi^*_{i\sigma}\psi_{i\sigma} - (\mu-\epsilon_i)\hat{n}_i + \frac{U_0}{2}\hat{n}_i(\hat{n}_i-1) + \frac{U_2}{2}(\mathbf{S}_i^2 - 2\hat{n}_i) \quad (7)$$

where $\phi_{i\sigma} = \sum_j \psi_{j\sigma}$. The sum j includes all nearest neighbors at the site i of a square lattice with $z = 4$, z being the coordination number.

Our main task is to find the SF order parameter, $\psi_{i\sigma}$ by diagonalizing the mean field Hamiltonian H_i^{MF} in Eq.(7) in the site occupation number basis, $|\hat{n}_{i\sigma}\rangle$. For that, we first have to find the matrix elements of H_i^{MF}, which is done via,

$$\langle\hat{n}_{i+},\hat{n}_{i0},\hat{n}_{i-}|H_i^{MF}|\hat{n}'_{i+},\hat{n}'_{i0},\hat{n}'_i\rangle = h_i^d + h_i^{od} \quad (8)$$

where the h_i^d part includes the matrix elements coming from the diagonal part of the mean field Hamiltonian and reads

as,

$$h_i^d = \Big[t\sum\nolimits_\sigma \phi^*_{i\sigma}\psi_{i\sigma} - (\mu-\epsilon_i)(n_{i+}+n_{i0}+n_{i-}) + \frac{U_0}{2}(n_{i+}+n_{i0}+n_{i-})(n_{i+}+n_{i0}+n_{i-}-1) + \frac{U_2}{2}\big(2n_{i+}n_{i0}+2n_{i+}n_{i0}+n_{i+}+2n_{i0}+n_{i-}+n_{i+}^2 - 2(n_{i+}+n_{i+}+n_{i+})\big)\Big]\delta_{n_{i+},n'_{i+}}\delta_{n_{i0},n'_{i0}}\delta_{n_{i-},n'_{i-}} \quad (9)$$

While the off diagonal part h_i^{od} is,

$$h_i^{od} = t\Big[\phi^*_{i+}\sqrt{n_{i+}}\delta_{n_{i+},n'_{i+}+1}\delta_{n_{i0},n'_{i0}}\delta_{n_{i-},n'_{i-}} + \phi^*_{i0}\sqrt{n_{i0}}\delta_{n_{i+},n'_{i+}}\delta_{n_{i0},n'_{i0}-1}\delta_{n_{i-},n'_{i-}} + \phi^*_{i-}\sqrt{n_{i-}}\delta_{n_{i+},n'_{i+}}\delta_{n_{i0},n'_{i0}}\delta_{n_{i-},n'_{i-}-1} + h.c\Big] + \frac{U_2}{2}\Big[\sqrt{n_{i0}(n_{i0}-1)(n_{i+}+1)(n_{i-}+1)}\,\delta_{n_{i+},n'_{i+}+1}\delta_{n_{i0},n'_{i0}-2}\delta_{n_{i-},n'_{i-}+1} + h.c\Big] \quad (10)$$

Hence we diagonalize the matrix in Eq.(8) to obtain the ground state energy $E_g^i(\psi_{i\sigma})$ and the eigenfunction $\Psi_g(\psi_{i\sigma})$ starting with some some guess value for $\psi_{i\sigma}$. Now from the updated wave function $\Psi_g(\psi_{i\sigma})$, we compute the SF order parameter using,

$$\psi_{i\sigma} = \langle\Psi_g(\psi_{i\sigma})|\hat{a}_{i\sigma}|\Psi_g(\psi_{i\sigma})\rangle \quad (11)$$

Using this new value of $\psi_{i\sigma}$, we again reconstruct the matrix and repeat the diagonalization procedure until self consistency condition is reached [28].

The variation of the equilibrium ground state energy, E_g with occupation number, n shows that it almost stabilizes corresponding to n=7, for which $\langle\hat{n}_{i+},\hat{n}_{i0},\hat{n}_{i-}|H_i^{MF}|\hat{n}'_{i+},\hat{n}'_{i0},\hat{n}'_i\rangle$ is a 120×120 matrix [see Fig.1]. The dimension is obtained by considering all possible combination of $\hat{n}_{i+}$, $\hat{n}_{i0}$, $\hat{n}_{i-}$ such that, $\hat{n}_{i+}+\hat{n}_{i0}+\hat{n}_{i-}$=$\hat{n}_i$. The local density, ρ_i and compressibility, κ_i can also be computed using,

$$\rho_i = \langle\Psi_g(\psi_{i\sigma})|\hat{n}_{i\sigma}|\Psi_g(\psi_{i\sigma})\rangle;\;\; \kappa_i = \langle\rho_i^2\rangle - \langle\rho_i\rangle^2 \quad (12)$$

In the clean state, that is when Δ/U_0=0, the mean field Hamiltonian is homogeneous and hence the SF order parameter is uniform throughout the entire lattice. In the strong interaction limit ($U_0 \gg t$), the SF order parameter vanishes indicating that the system is in the MI regime where the atoms are forbidden from tunneling into neighbouring sites and thereby are localized to individual sites with a fixed number of bosons per site. Thus the MI phase is characterized by zero SF order parameter and zero compressibility with a finite gap in the particle hole excitation spectrum.

In the weak interaction limit ($t \gg U_0$), the SF order parameter shows finite value whence the atoms can easily tunnel between the nearest neighbour sites. In the superfluid phase, atoms are delocalized over the entire lattice and the ground state is a coherent state, which in experiments is seen to form a constructive interference pattern in the momentum space. Thus the superfluid phase is characterized by non zero order parameter, non integer boson density and finite compressibility with no particle hole excitation gap in the spectrum.

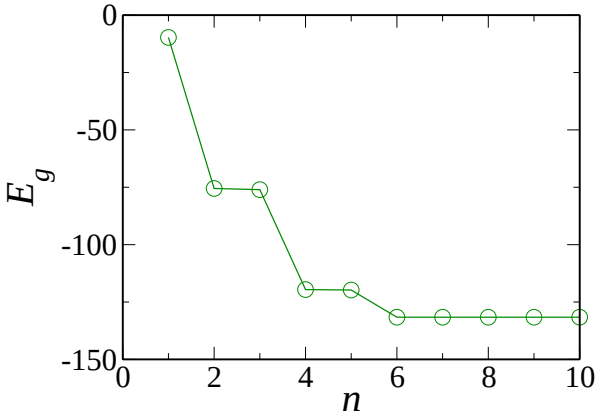

FIG. 1. The variation of the equilibrium ground state energy, E_g with occupation number n.

In presence of disorder, the mean field Hamiltonian becomes inhomogeneous and hence the SF order parameter will vary from one site to another. Further, in the pure case, the system can make direct phase transition from MI to SF phase controlled by the system parameter t and U_0. But as soon as disorder is present, the BG phase always intervenes between the SF and MI phases. The BG phase is defined as the zero SF order parameter with no gap in the particle hole excitation spectra. Thus the three types of phases can be characterized as,
(i) SF phase: $\psi_i \neq 0$, $\rho_i \neq$integer and $\kappa_i > 0$
(ii) BG phase: $\psi_i = 0$, $\rho_i \neq$ integer and $\kappa_i > 0$
(iii) MI phase: $\psi_i = 0$, $\rho_i =$integer and $\kappa_i = 0$

In order to see the effects of disorder, we first solve our mean field Hamiltonian, Eq.(7) self consistently on a two dimensional (2D) square lattice of size $L\times L$ where we have considered $L = 30$ throughout our calculations (unless mentioned otherwise) to obtain the averaged value of $\bar{\psi}$ and $\bar{\rho}$ as,

$$\bar{\psi} = \Big[\frac{1}{L^2}\sum_{i=1}^{L^2}\psi_i\Big]_{sample} \;\; and \;\; \bar{\kappa} = \Big[\frac{1}{L^2}\sum_{i=1}^{L^2}\kappa_i\Big]_{sample} \quad (13)$$

where sample in the subscript refer to the fact that results are averaged over different realizations of disorder. Here we have used a maximum of 40 different disorder realizations and confirmed that the fluctuations are satisfactorily equilibriated.

III. RESULTS

In this section we shall present our results by numerically solving the mean field Hamiltonian, Eq.(8) in the $zt-\mu$ plane while keeping U_0=1 and considered different values of spin dependent interaction U_2. Since $U_2/U_0=(a_2-a_0)/(a_0+2a_2)$, so U_2/U_0 extends from -1 when a_2=0 to 0.5 when a_0=0. In our work, we choose U_2/U_0=0.1 (less than the maximum value 0.5) to study the odd and even MI lobes. It may be noted that at $U_2/U_0 \geq 0.5$, the odd MI lobes are completely consumed by the even MI lobes. For the ferromagnetic case, any value of U_2 in the interval [-1, 0] is seen to yield qualitatively similar results and we choose U_2/U_0=-0.2.

The other important parameter is the disorder strength, Δ/U_0. Since the MI phase is characterized by finite energy gap in their energy spectrum, in the atomic limit (t=0) the width for the MI lobe is energy gap between the upper and lower values of the chemical potential, μ corresponding to the particle and hole excitations [36]. In the antiferromagntic case, the width of the odd MI lobes is $E_g=\mu_+-\mu_-=U_0-2U_2$, while for the even MI lobes, it is $E_g=U_0+2U_2$ [37]. In order to go from a gapped MI phase to a gappless BG phase, the disorder strength, Δ/U_0 should be greater or equal to the width of the respective MI lobes. Since we are using a box disorder from -Δ to Δ, so the critical disorder strength, Δ_c should extend from -$E_g/2$ to +$E_g/2$ that is Δ_c/U_0=0.4 for the odd MI lobes and Δ_c/U_0=0.6 for the even MI lobes corresponding to U_2/U_0=0.1. Similarly for the ferromagnetic case, the energy gap corresponds to $E_g=U_0+U_2$ and hence the critical value is Δ_c/U_0=0.4 corresponding to U_2/U_0=-0.2. Using this parameter values, we shall present our results systematically in the following.

A. The behaviour of the SF order parameter and compressibility

In this section we present our results of the averaged order parameter, $\bar{\psi}$ and compressibility, $\bar{\kappa}$ to characterize the MI, BG and SF phases as a function of tunneling strength zt/U_0. In the pure case, the $\bar{\psi}$ and $\bar{\kappa}$ undergo a transition from zero to finite values indicating a direct MI-SF transition. That is, the system remains in the MI phase as long as the tunneling strength, t is well below the critical tunneling strength t_c, where the latter is given by [38],

$$zt_c=(1/3)(U_0+2U_2)[(2\rho+3)-\sqrt{4\rho^2+12\rho}] \qquad (14)$$

While in the disordered case, the BG phase appears and it tries to displace the MI phase making inroads for itself. The behaviours of $\bar{\psi}$ and $\bar{\kappa}$ in both antiferromagnetic and ferromagnetic regions is discussed below.

(i) Antiferromagnetic case: The spin dependent interaction, U_2 for ^{23}Na is antiferromagnetic since the atomic scattering length $a_2 > a_0$. For $U_2/U_0 > 0$, the nature of MI-SF phase transition is either of second or first order corresponding to the MI lobes with odd or even local densities respectively, while for a scalar Bose gas, it is always a second order phase transition.

In the Mott insulating phase, with an odd value for the local density per site, the SF order parameter, $\bar{\psi}$ and the compressibility, $\bar{\kappa}$ changes continuously from zero, thereby indicating a second order MI-SF phase transition. However, the MI phase with each site having even local density, the $\bar{\psi}$ and $\bar{\kappa}$ show finite jumps indicating the first order MI-SF phase transition [19], [39].

We have also found that the three SF order parameters assume the values, such as $\psi_{i+}=\psi_{i-}\neq 0$ and $\psi_{i0}=0$ in the MI phase making the ground state only functions of ψ_{i+} and ψ_{i-} and hence the equilibrium value of the total spin is $\langle \mathbf{S}\rangle^2=0$, which is responsible for making the SF phase a polar state [19], [20].

In order to visualize the different kinds of phase transition corresponding to the MI lobes with different occupation densities, we plot $\bar{\psi}$ and $\bar{\kappa}$ in the pure and disordered cases. We choose the values of μ in such a way so that we are at the MI lobes with local density ρ_i=odd and even. At μ/U_0=0.4, we are in the vicinity of the odd MI lobe with the local density $\rho_i=1$ while for $\mu/U_0=1.4$, the local density comes out as ρ_i=2 implying we are at the even MI lobe.

In the pure case, we found that corresponding to U_2/U_0=0.1, the system remains in the Mott insulating phase with $\bar{\psi}$ and $\bar{\kappa}$ as zero till zt/U_0=0.16 for the first odd MI lobe at μ/U_0=0.4 and zt/U_0=0.26 for the first even MI lobe at μ/U_0=1.4, both of which lie below the critical tunneling strength zt_c/U_0. Beyond this critical value, the system goes to a superfluid phase with non integer local densities, $\bar{\rho}$ and finite values of $\bar{\psi}$ [see Fig.2 (solid (black) lines)].

We shall now include the on-site disorder, ϵ_i and see how it affects the averaged SF order parameter and compressibility. The inclusion of ϵ_i can equivalently be treated as a site dependent chemical potential, μ_i ($\mu_i=\mu-\epsilon_i$). Since the SF order parameter and local densities become explicitly site dependent, it is impossible to determine the sharp value of the tunneling strength, zt for which a MI-BG transition can be observed. The variation of averaged SF order parameter $\bar{\psi}$ and $\bar{\kappa}$ for both the odd and even MI lobes for two different disorder strengths are shown in Fig.[2] at Δ/U_0=0.3 (dotted (red) lines) and Δ/U_0=0.5 (dashed (green) lines).

For the odd MI lobes, we found that the MI region starts to shrink due to appearance of the BG phase [see Figs.2(a) and 2(b)] and the region spanned by the MI phase gradually decreases at the larger value of the disorder strength. When the disorder strength exceeds the critical value of disorder for the respective MI lobes, the BG phase completely destroys the MI phase, resulting in only the existence of the BG and SF phases as pointed out earlier. Thus at Δ/U_0=0.5, the BG region extends till $zt/U_0 \simeq 0.072$ as perceived from the vanishing of the average SF order, $\bar{\psi}$ below 0.1 and finite average compressibility, $\bar{\kappa}$.

We also study the behavior of even MI lobes in the antiferromagnetic case at different disorder strengths. In the pure case, we choose μ/U_0=1.4 and we found that

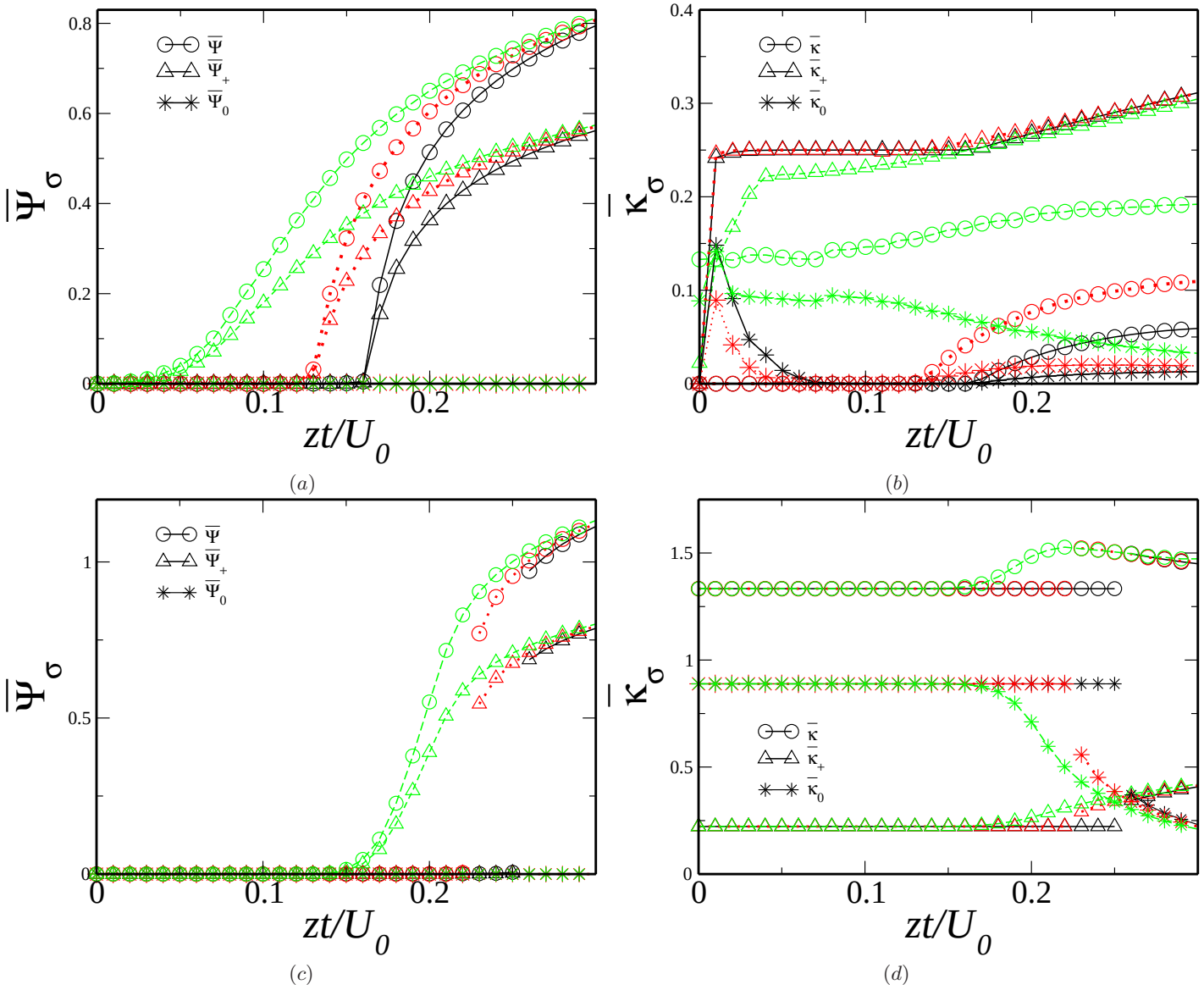

FIG. 2. (Color online) The variation of $\bar{\psi}_\sigma$ and $\bar{\kappa}_\sigma$ at $U_2/U_0 = +0.1$ (antiferromagnetic) with disorder strengths $\Delta/U_0 = 0.3$ (dotted (red) lines) and 0.5 (dashed (green) lines) respectively and $\bar{\psi}_+ = \bar{\psi}_-$, $\bar{\kappa}_+ = \bar{\kappa}_-$ and $\bar{\psi}_0 = \bar{\kappa}_0 = 0$. The pure case ($\Delta/U_0 = 0$) is included for comparison (solid (black) lines). At $\mu/U_0 = 0.4$, $\bar{\psi}$ and $\bar{\kappa}$ show continuous variations indicating a second order phase transition for MI lobes with $\rho = 1$ [(a) and (b)]. While at $\mu/U_0 = 1.4$, $\bar{\psi}$ and $\bar{\kappa}$ show continuous variation indicating a second order transition for MI lobes with $\rho = 2$ at Δ/U_0=0.5. [(c) and (d)].

both $\bar{\psi}$ and $\bar{\kappa}$ show jumps from zero and a constant value respectively to distinct finite values signaling the first order phase transition for the even MI lobes [see Figs.2(c) and 2(d) (solid (black) lines)]. In presence of disorder, the MI state starts to diminish due to the appearance of the BG phase and the MI-SF phase transition continues to be first order for Δ/U_0=0.3 [see Figs.2(c) and 2(d) (dotted (red) lines)]. While at Δ/U_0=0.5 [see Figs.2(c) and 2(d) (dashed (green)lines)], the MI state still survives but the MI-SF transition becomes a second order phase transition.

We have also investigated the behaviour of the individual SF order parameter and local density components at different disorder strengths at both values of chemical potential, namely μ/U_0=0.4 and 1.4. At Δ/U_0=0, it is found that the SF order parameters behave as, ψ_+=ψ_-=ψ_0=0 with the occupation densities becoming ρ_+=ρ_- $\simeq$ 0.5 and ρ_0 $\simeq$ 0 at μ/U_0=0.4 and ρ_+=ρ_-=ρ_0=2/3 at μ/U_0=1.4 in the MI phase. While ψ_+=ψ_- $\neq$ 0, ψ_0=0 and ρ_+, ρ_-, ρ_0 behave similar to that of ρ in the SF phase satisfying the condition ρ=$\sum_\sigma \rho_\sigma$ and correspondingly $\bar{\psi}_\sigma$ and $\bar{\kappa}_\sigma$ at Δ/U_0=0.3, 0.5 are shown in Fig.[2]. The compressibility, $\bar{\kappa}_\sigma$ is constant in the MI phase and gradually increases in the SF phase for even MI lobes.

The above scenario is equivalent to the MI phase with fractional occupation densities for an individual spinor components, although the summed over spinor components yields an integer.

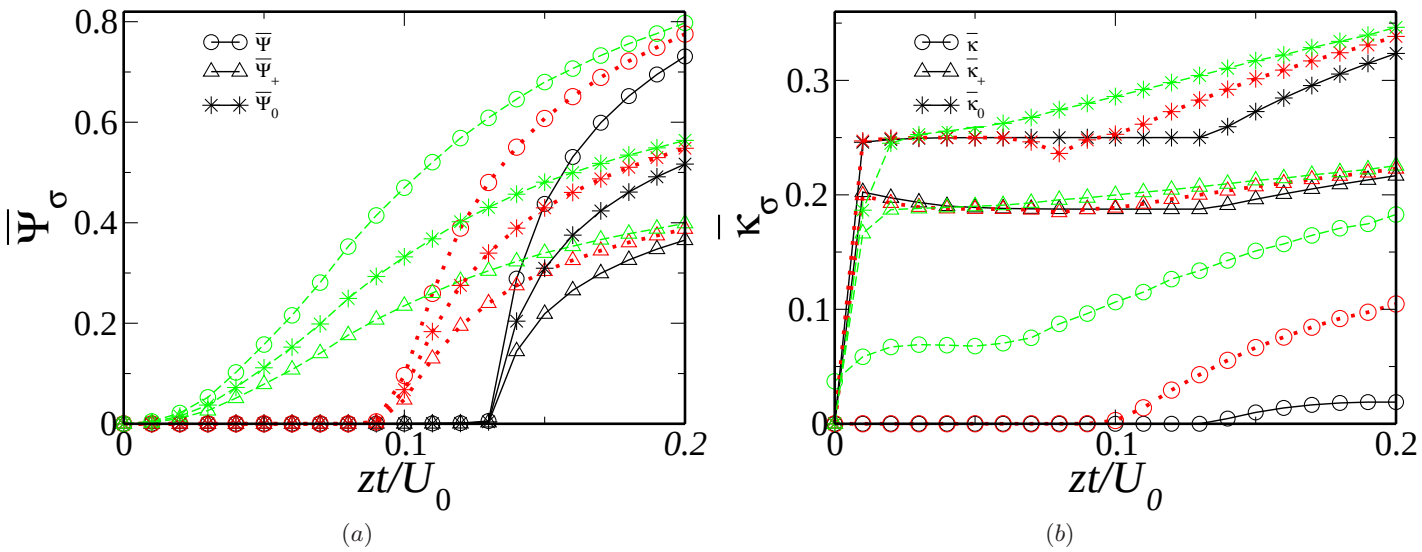

FIG. 3. (Color online) The variation of $\bar{\psi}_\sigma$ and $\bar{\kappa}_\sigma$ at U_2/U_0=-0.2 (ferromagnetic) with disorder strengths $\Delta/U_0 = 0.3$ (dotted (red) lines) and 0.5 (dashed (green) lines) respectively and $\bar{\psi}_+$=$\bar{\psi}_-$, $\bar{\kappa}_+$=$\bar{\kappa}_-$. The pure case ($\Delta/U_0 = 0$) is included for comparison (solid (black) lines). At $\mu/U_0 = 0.4$, $\bar{\psi}$ and $\bar{\kappa}$ show continuous variation indicating a second order phase transition for MI lobes with $\rho = 1$ [(a) and (b)]

(ii)Ferromagnetic case: For ^{87}Rb atoms, the experimental data yield $a_2 < a_0$ for the scattering lengths in the respective channels for which the spin dependent interaction $U_2 \leq 0$ and the spin-1 ultracold atoms show similar behavior as that of scalar or spinless Bose gas where the MI-SF phase transition is now a second order one.

In the ferromagnetic regime, all the three components of the SF order parameter are non zero in the SF phase and the ground state is now functions of ψ_{i+}, ψ_{i-}, ψ_{i0}. In the pure case, we found that $\psi_{i+} = \psi_{i-}$ and $\psi_{i0} = \sqrt{2}\psi_{i+}$ and the total spin operator $\langle \mathbf{S} \rangle^2$ in the superfluid phase now only takes the value of unity which confirms that we have a ferromagnetic superfluid state [19], [20].

The variation of $\bar{\psi}$ and $\bar{\kappa}$ are shown in Figs.[3(a) and 3(b)] for both pure and disordered cases at $U_2/U_0 = -0.2$ and $\mu/U_0 = 0.4$. When $\Delta/U_0 = 0$, the local density, $\rho = 1$ and $\bar{\psi}$, $\bar{\kappa}$ are zero till zt/U_0=0.13 ($< zt_c$) indicating the system is in the MI regime. As zt/U_0 increases, the system smoothly goes toward the SF regime with finite $\bar{\psi}$ and $\bar{\kappa}$ and non integer local densities [see Figs.3(a) and 3(b) (solid (black) lines)].

As disorder is introduced, the BG phase intervenes in between the MI and SF phases. Thus the width of the MI phase at a disorder strength, Δ/U_0=0.5 [see Figs.3(a) and 3(b) (dashed (green) lines)] becomes much lesser as compared to that of Δ/U_0=0.3 [see Figs.3(a) and 3(b)(dotted (red) lines)]. From Fig.[3], we see that at Δ/U_0=0.5, the region spanned by the MI phase is completely occupied by the BG phase, resulting in only the survival of the BG and the SF phases owing to similar reasons as that of the antiferromagnetic case discussed earlier.

We also study the behavior of the individual SF order parameter and local density components at different disorder strengths at μ/U_0=0.4. At Δ/U_0=0, ψ_+=ψ_-=ψ_0=0 and ρ_+=ρ_- $\simeq$ 0.25 and $\rho_0 \simeq 0.5$. The compressibility, $\bar{\kappa}_\sigma$ is constant in the MI phase and corresponding $\bar{\psi}_\sigma$ and $\bar{\kappa}_\sigma$ at Δ/U_0=0.3, 0.5 are shown in Figs.[3(a)and 3(b)].

B. Indicators of MI, BG and SF phases

In the previous section we have studied the effects of onsite disorder on the averaged SF order parameter and the compressibility. Since we have averaged the SF order parameter and the compressibility, it becomes very difficult to locate the precise parameter values for a MI-BG and BG-SF transition, owing to the fact that the ψ_i and the ρ_i are explicitly site dependent. Thus at the transition point there are some sites with zero SF order parameter and integer occupation densities, while other sites may have zero SF order parameter and non integer occupation densities.

In order to circumvent this difficulty, we define a measurable quantity, χ which is defined as,

$$\chi = \frac{Sites\ with\ \psi_i \neq 0\ \ and\ \rho_i \neq integer}{Total\ numbers\ of\ sites} \qquad (15)$$

In a similar manner, we can also define the χ_σ involving $\psi_{i\sigma}$ and $\rho_{i\sigma}$ which will aid in the study of the individual spinor components.

The main reason to define χ is to distinguish between the MI, BG and SF phases where depending upon the value of χ, we will be able to easily characterize the three different types of phases.

At this point, one can ask, what will be the value of ψ_i and ρ_i which can define the MI or the SF phase. Since we see from the behaviour of $\bar{\psi}$ and $\bar{\kappa}$ in the pure case that the system will remain in the MI phase till $zt < zt_c$ having vanishingly small $\psi_{i\sigma}$ (values below $O(10^{-2})$) and the occupation density $\rho_i = N \pm \delta$ where $N = 0, 1, 2, 3...$ and δ is of $O(10^{-3})$. These values are set for numerical

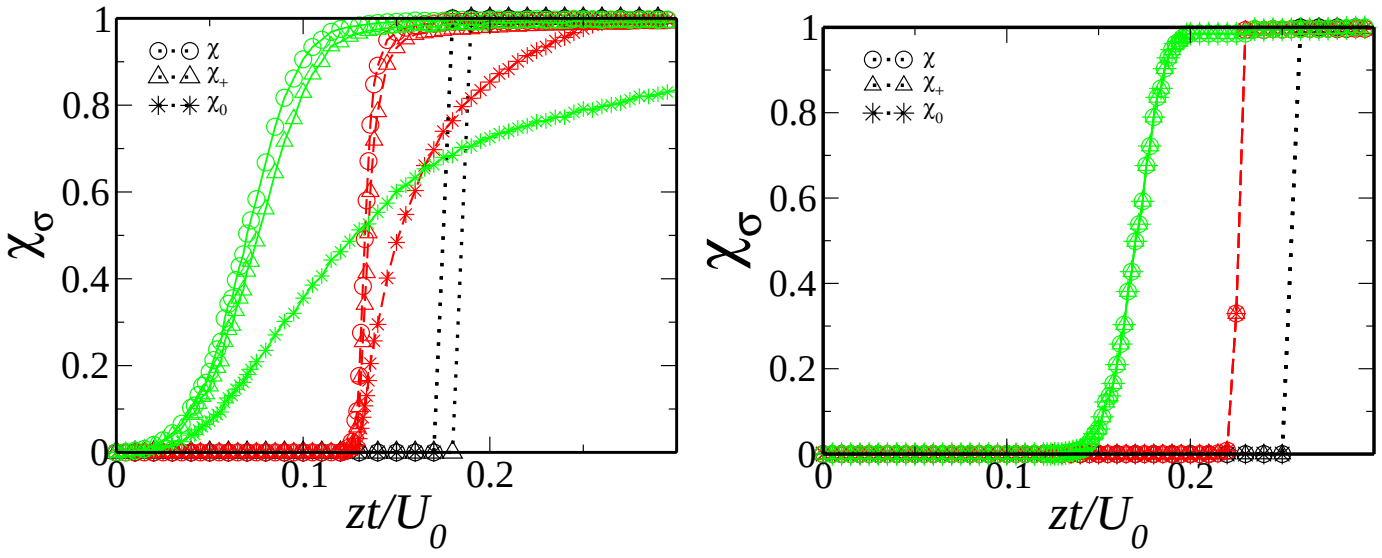

FIG. 4. The variation of χ_σ in the antiferromagnetic case with U_2/U_0=+0.1 for both the odd and even MI lobes corresponding to the pure case Δ/U_0=0.0 (dotted (black) lines) and for disordered values, Δ/U_0=0.3 (dashed (red) lines) and 0.5 (solid (green) lines) respectively. χ_σ for odd MI lobe at μ/U_0=0.4 is shown in (a) while for the even MI lobes at μ/U_0=1.4 in (b).

convergence of the parameters corresponding to the MI phase. Again as earlier, we include discussion of the antiferromagnetic and ferromagnetic regimes one by one.

(i) Antiferromagneic case: For antiferromagnetic interaction with U_2/U_0=0.1, we study the the variation of χ with tunneling strength, zt/U_0 in both pure and disordered cases at two different values of μ/U_0 corresponding to the odd and even MI lobes respectively as shown in Fig.[4].

In the disorder free case for μ/U_0=0.4, we see that χ makes direct transition from 0 to 1 emphasizing an unhindered MI-SF transition. When $zt < zt_c$, the system is in MI phase, that is all sites have ψ_i=0 and ρ_i=integer and thus χ takes the value 0. While for $zt > zt_c$, the system becomes a SF phase with $\psi_i \neq 0$ and $\rho_i \neq$ integer and thereby χ assumes a value 1 [see Fig.4(a) (dotted (black) lines)]. As soon as disorder is included, the direct transition of χ from 0 to 1 is prohibited indicating a gradual increase due to the presence of the BG phase.

In presence of disorder, that is at Δ/U_0=0.3 [see Fig.4(a) (dashed (red) lines)], χ remains zero till $zt/U_0 = 0.133$, beyond which χ starts to increase indicating that some sites with ρ_i=integer in the MI regime start evolving and the system move towards the BG regime with $\rho_i \neq$ integer. Further, the gradual increase of the slope of χ refers the intrusion of the BG phase into a territory which used to be the MI phase without disorder. As disorder strength increases, that is at Δ/U_0=0.5 [see Fig.4(a) (solid (green) lines)], we see that χ only takes finite values and ultimately go unity as a function of zt/U_0, indicating that the region spanned by the BG phase continues to increase and results in vanishing of the MI phase. Thus at Δ/U_0=0.5, the system only consists of the BG and SF phases as expected since the disorder strength Δ/U_0 exceeds the energy gap for the first odd MI lobe (ρ=1).

It is now quite interesting to study the behavior of χ_σ incorporating the effects of disorder. In order to study χ_σ, we use $\psi_{i\sigma}$ and $\rho_{i\sigma}$ and remember that they satisfy the same condition as the total SF order parameter, ψ_i and the local density, ρ_i for rendering the MI and the SF phases respectively.

At μ/U_0=0.4, the system is in the MI regime since the SF order parameter ψ_i ($=\sqrt{\psi_{i\sigma}^2}$) is small and the local densities are as, ρ_i=1, ρ_{i+}=$\rho_{i-} \simeq 0.5$, $\rho_{i0} \simeq O(10^{-3})$. Hence following the definition of χ, we compute $\chi_\pm$ by suitably modifying the numerator of the Eq.(16) with $\psi_{i\pm} \neq 0$ and $\rho_{i\pm} \neq 0.5$ respectively. In Fig.[4(a)], we have plotted $\chi_\pm$ with zt/U_0. We find that χ_+=χ_- where they show same behaviour as that of χ in the clean and disordered cases.

In the antiferromagnetic case, ψ_{i0} is always zero and ρ_{i0} behaves as $\rho_\pm$ corresponding to the MI and SF regimes respectively. So for determining χ_0, we set the condition ψ_{i0}=0 and $\rho_{i0} > 0.001$ in the numerator of Eq.(16). Its variation with respect to zt/U_0 is also shown in the Fig.[4(a)].

Similar to the discussion above, at μ/U_0=1.4, in the MI regime, the local densities yield an even MI lobe with ρ_i=2, ρ_{i+}= ρ_{i-}=ρ_{i0}=2/3 $\pm$ δ. So we compute $\chi_\pm$ by replacing the numerator of the Eq.(16) with $\psi_{i\pm} \neq 0$ and $\rho_{i\pm} \neq 0.667 \pm \delta$. For computing χ_0, we set the condition ψ_{i0}=0 and $\rho_{i0} \neq 0.667 \pm \delta$ respectively. The variation of χ and χ_σ with different disorder strengths are shown in Fig.[4(b)].

From the behaviour of χ, we see that at Δ/U_0=0.3 [see Fig.4(b)(dashed (red) lines)], although there is little value in between 0 and 1, but the region occupied by the MI phase shrinks as compared with the pure case [see Fig.4(b) (dotted (black) lines)], owing to the emergence of the BG

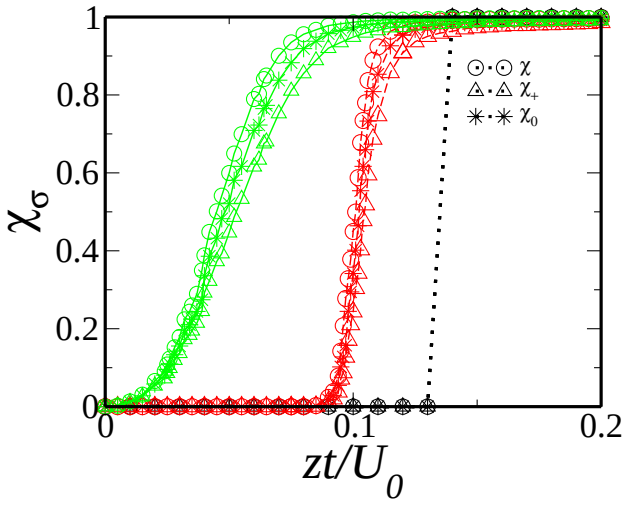

FIG. 5. The variation of χ_σ in the ferromagnetic case with U_2/U_0=-0.2 corresponding to the pure case Δ/U_0=0.0 (dotted (black) lines) and for disordered values, Δ/U_0=0.3 (dashed (red) lines) and 0.5 (solid (green) lines) respectively.

phase. For Δ/U_0=0.5 [see Fig.4(b) (solid (green) lines)], the BG phase appears as χ takes finite values in between 0 and 1, while the MI phase still exists since the critical disorder strength, Δ_c/U_0 for the ρ=2 MI lobe is a much higher as discussed in the previous section. Components of χ_σ show similar kind of behavior as that of χ in presence of disorder.

(ii)Ferromagnetic case: For ferromagnetic interactions with U_2/U_0=-0.2 at μ/U_0=0.4, the variation of χ_σ with tunneling strength zt/U_0 is shown in Fig.[5]. In the ferromagnetic case, since the spin-1 ultracold atoms shows similar phase diagram as that of a scalar Bose gas (spinless), so there is no distinction between the odd and the even MI lobes, and thus showing results involving either will suffice.

At μ/U_0=0.4, the MI lobes has local density ρ_i=1 and χ is zero till zt/U_0=0.133. Beyond this value, the system goes to the SF phase with χ=1 in the pure case [see Fig.5 (dotted (black) lines)]. In presence of disorder, that is at Δ/U_0=0.3 [see Fig.5 (dashed (red) lines)], χ remains zero till zt/U_0=0.085, beyond which χ starts to increase and at Δ/U_0=0.5 [see Fig.5 (solid (green) lines)] χ only takes the value between 0 and 1 indicating that the system only consists of the BG and SF phases. In the latter case, disorder completely annihilates the MI phase because the disorder strength crosses the critical disorder value, Δ_c/U_0=0.4.

At μ/U_0=0.4, in the MI regime, the SF order parameter, ψ_i $(=\sqrt{\psi_{i\sigma}^2})$ is small and the local densities are given by ρ_i=1, ρ_{i+}=ρ_{i-}=0.25 $\pm$ δ, ρ_{i0}=0.5 $\pm$ δ. We compute the $\chi_{\pm,0}$ by modifying the Eq.(16) with $\psi_{i\pm,0} \neq 0$ and $\rho_{i\pm,0}$ respectively, since in the SF regime, all the three SF spinor components are finite. In Fig.[5] we have plotted $\chi_{\pm,0}$ as a function of zt/U_0 which show same behaviour as that of χ in both the clean and disordered cases.

C. Percolation analysis and finite size scaling

At this point we will try to figure out one of our earlier questions that was posed in this regard, whether is it possible to locate the transition point for the MI-BG transition in the presence of disorder with confidence. Further what will be the extent of the BG phase, that is, whether the whole region is a BG phase or there is certain amount of SF phase still left in presence of disorder. To answer the questions we have to really look at the concept of the appearance of percolating cluster of sites with non integer occupation densities and finite SF order parameter. In order to understand what do we mean by a percolating cluster, we have shown the typical real space plots of ψ_i and ρ_i for three different values of zt/U_0 corresponding to the three different phases of the system in Fig.[6]. The pair of figures shown in each column depicts MI [see Fig.6(a)], BG [see Fig.6(b)] and SF [see Fig.6(c)] phases. The top and bottom plots in each of them illustrate the values of SF order parameter, ψ_i and the local density ρ_i respectively in a square lattice of size $L \times L$=50 $\times$ 50 for a single realization of the disorder. The parameter corresponding to the plots are Δ/U_0=0.5 and μ/U_0=0.4 in the antiferromagnetic case (U_2/U_0=+0.1). The light green circles are the indicators for the zero SF order parameter and the integer densities, while the deep red circles denote non zero SF order parameter and non integer densities. The ψ_i and ρ_i for the MI phase at zt/U_0=0.001 and for the BG phase at zt/U_0=0.06 and for the SF phase at zt/U_0=0.3.

In the clean state, the system splits into two, the MI islands with all sites having zero ψ_i and integer densities ρ_i as shown by light dots in Fig.[6(a)] till $zt/U_0 < zt_c/U_0$ and the SF islands with finite ψ_i and non integer densities ρ_i at $zt/U_0 > zt_c/U_0$ separated by a sharp boundary. As soon as disorder is introduced, the BG phase tries to mix two islands by removing the boundary between them. So the sites with zero ψ_i and integer densities attempt to evolve towards zero ψ_i and non integer densities as shown in Fig.[6(b)] (BG phase), which finally percolates for the first time towards a state with non zero ψ_i and non integer densities Fig.[6(c)], the latter being the SF phase.

To extract different phases of the system, we shall concentrate on the appearance of the SF clusters which percolate throughout the entire lattice for the first time. In the MI states, all sites have integer particle densities and hence there will be no SF cluster, while in the BG phase, some of the sites have non integer densities and thus the SF clusters will be trapped by other clusters with sites having integer densities. Finally with the increase in the tunneling strength, the SF clusters will start to percolate throughout the lattice resulting in a SF phase for the system. Thus the BG region can be identified in between the MI and the SF phases where SF clusters exist, however do not percolate across the lattice.

When a SF cluster percolates through an infinite lattice it is known as an infinite cluster, while when it percolate through a finite lattice it is known as a percolating or

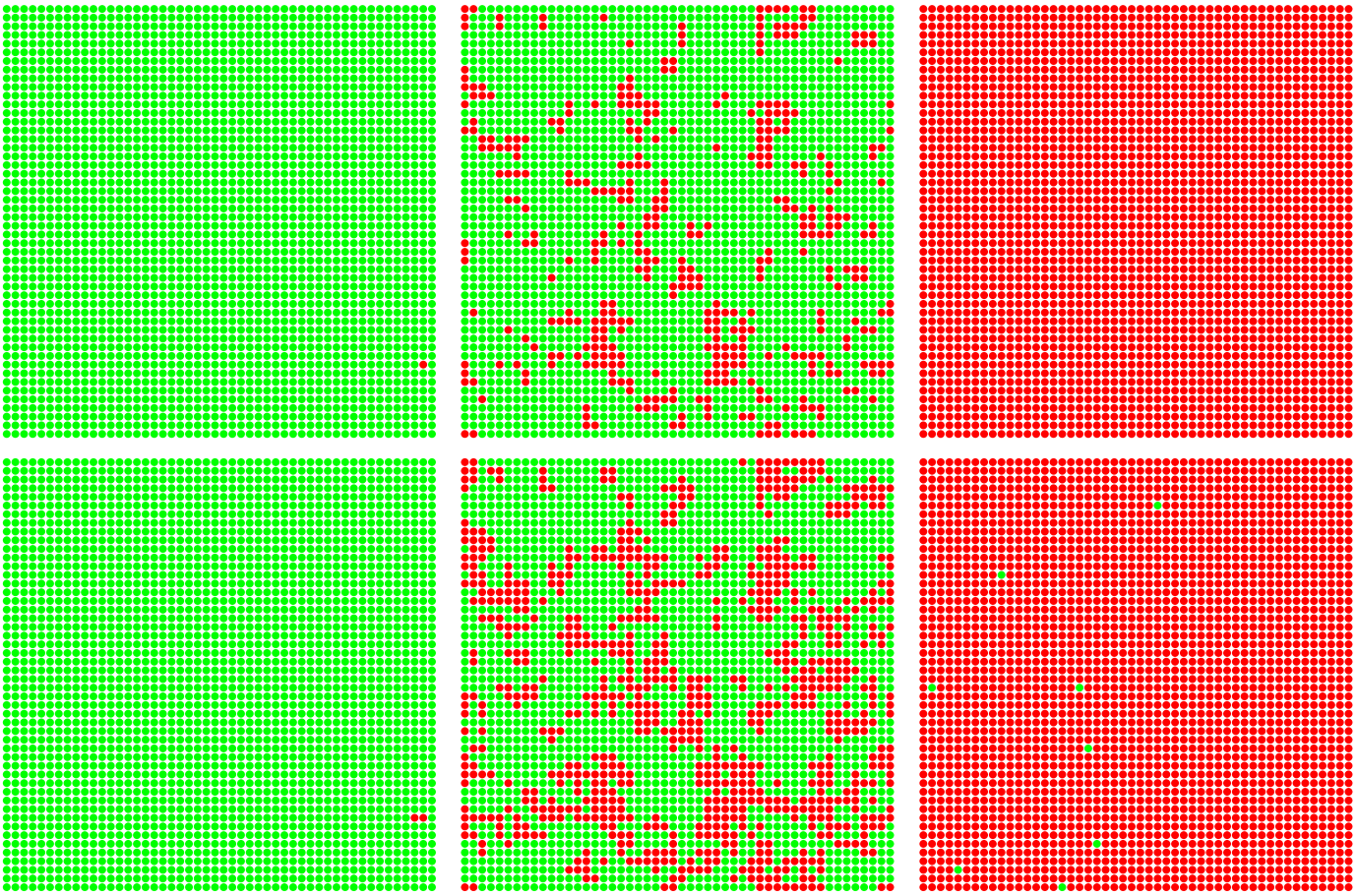

FIG. 6. (color online) The real space plots of SF order parameter, ψ_i (first row) and the occupation densities, ρ_i (second row) for lattice size $L \times L$=50 × 50 at Δ/U_0=0.5 with U_2/U_0=+0.1 and μ/U_0=0.4 corresponding to three different phases that is the MI, BG and SF phases of the system respectively. The light green circles (light shades) represent the zero SF order parameter and integer densities and deep red circles (deep shades) represent the non zero SF order parameter and non integer densities. The parameter value is at zt/U_0=0.001 in the MI phase (a) and zt/U_0=0.06 in the BG phase (b) and zt/U_0=0.3 for the SF phase (c) respectively.

spanning cluster. Since we are dealing with a finite size of the system for our numerical work, we shall aim to find a spanning cluster using HK algorithm [30].

Whether a SF cluster will percolate can be well understand from the following quantity, χ_∞ which is defined as [40],

$$\chi_\infty = \frac{Sites\ in\ a\ spanning\ cluster}{Total\ number\ of\ occupied\ sites} \tag{16}$$

Here we briefly outline the idea used in the HK algorithm for the sake of completeness. It is based on the special application of the union-find algorithm where it aims to assign a label to each cluster. For that, we represent our 2D lattice as a matrix and label all occupied sites initially with -1 and unoccupied sites with 0. Our cluster index starts with 1. Corresponding to each occupied site, every time we check the neighbours at the top and left corner of the current site. If both sites are empty, we label a new cluster number that has not used so far. Else, if the site has one occupied neighbour, then we assign same cluster number to the current site. If both neighbouring sites are occupied, then we set the smallest number cluster label of the occupied neighbours to use as the label for the current site. To link two clusters, we create a union between both labels and set the site as the lowest of the two labels. When we burn the lattice for a second time, we collect the unions and update the lattice.

In Fig.[7(a)] we study χ_∞ as a function of χ at a disorder strength Δ/U_0=0.5 and μ/U_0=0.4 in the antiferromagnetic case. It is found that χ_∞ is zero till χ=χ_c=0.581 for a lattice size $L \times L$ =128 × 128 which is close to the critical threshold value for the occupation probability p_c=0.592 for random site percolation problem in an infinite 2D square lattice [40] and shows finite value above $\chi > \chi_c$. These similarity is only coincidental as the random site percolation model is a classical problem where sites are randomly occupied, while we have a system of quantum particles and the driving parameters are systematically varied at a given value of random disorder.

Another useful quantity in this regards, is the mean clus-

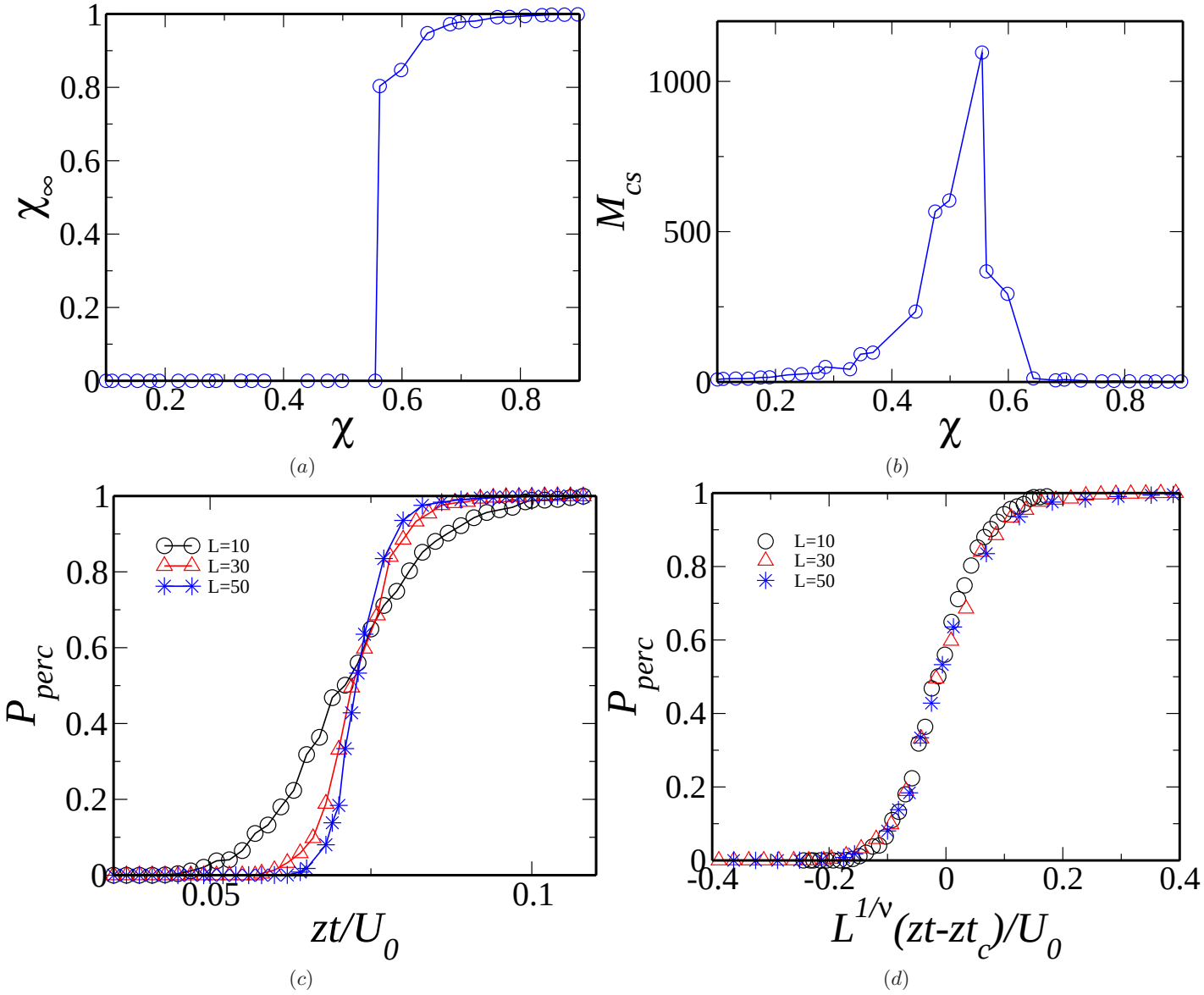

FIG. 7. (Color online) The percolation probability, χ_∞ and the mean cluster size, M_{cs} corresponding to a lattice size $L\times L$=128×128 at Δ/U_0=0.5 for the antiferromagnetic case with U_2/U_0=+0.1 and μ/U_0=0.4 are shown in (a) and (b). The percolation probability, P_{perc} corresponding to different lattice size L with system parameter, η=zt/U_0 and finite size scaling are shown in (c) and (d). The critical tunneling strength η_c where P_{perc} for different L values intersect at η_c=zt_c/U_0=0.073.

ter size, M_{cs} defined as [40]-

$$M_{cs}(\chi) = \frac{\sum_p^\infty p^2 s_p(\chi)}{\sum_p^\infty p s_p(\chi)} \tag{17}$$

where ps_p is the number of occupied sites belonging to a *p-th* cluster and the spanning clusters are excluded from the sum. Since the spanning clusters are excluded from the sum, the mean cluster size continues to increase with χ till the appearance of a spanning cluster for the first time and starts to decay immediately after that. The variation of M_{cs} with χ at a disorder strength Δ/U_0=0.5 for μ/U_0=0.4 [see Fig.7(b)] shows that it reaches its peak value just below the χ_c and falls off after χ_c which confirms that the system is in the BG phase till χ_c, and beyond that it goes toward the SF phase.

To deal with the finite size effects and also to determine the percolation transition, we resort to the finite size scaling. For a given system size L, we shall now study the percolation probability P_{perc} which is the probability of having a percolating cluster with the system parameter η=zt/U_0. Fig.[7(c)] shows the variation of P_{perc} with different lattice sizes L at a particular disorder strength, Δ/U_0=0.5 and μ/U_0=0.4 in the antiferromagnetic case. We averaged our results over 1000 (L=10) and 100 (L=30, 50) different realizations of disorder. The P_{perc} is assumed to follow a scaling law near the critical tunneling strength, η_c [40] and is described by,

$$P_{perc}(L,\eta) = \tilde{p}(L^{\frac{1}{\nu}}(\eta-\eta_c)) \tag{18}$$

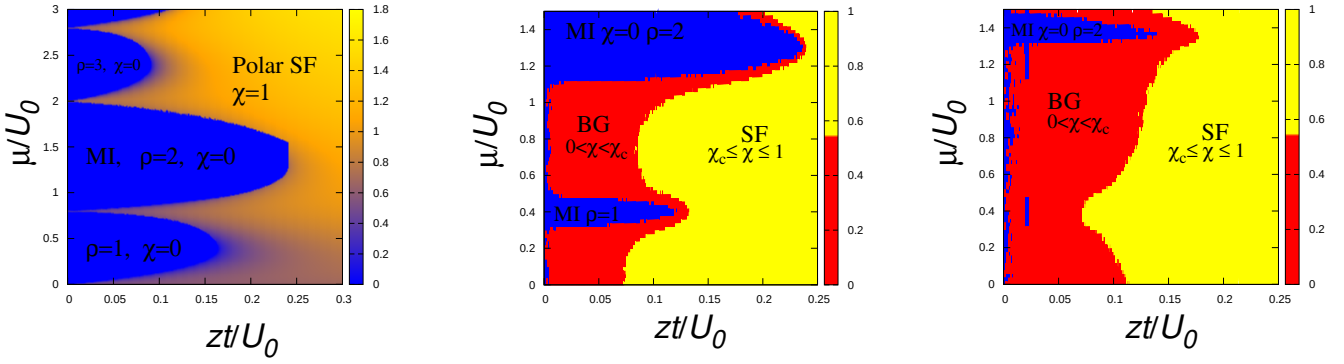

(a) (b) (c)

FIG. 8. (Color online) Phase diagram of spinor ultracold atoms in $t-\mu$ plane at U_2/U_0=+0.1 (antiferromagnetic). In the pure case (Δ/U_0=0.0), the odd MI lobes start to shrink while the even MI lobes expanded and the colour variation corresponds to the magnitude of the SF order parameter ψ shown in the legend of (a). Phase diagram based on the information obtain from χ for the disordered cases, namely Δ/U_0 =0.3 is shown in (b) and Δ/U_0=0.5 in (c).

where P_{perc} for different L values intersect approximately at one critical point given by η_c=zt_c/U_0 and $\tilde{p}$ is the scaling function which approaches zero in $(\eta-\eta_c) << 0$ and unity for $(\eta-\eta_c) >> 0$, ν is the critical exponent which is equal to 1.33 for conventional random site percolation problem in two dimension. The finite size scaling plot, where all data corresponding to different system sizes collapse on a single curve, is shown in Fig.[7(d)] where the corresponding critical tunneling strength is given by η_c=zt_c/U_0=0.073. For the sake of brevity we have not included the discussion corresponding to the ferromagnetic case.

We are now in a position to distinguish the three different types of phases and able to ascertain the critical tunneling strength, η_c=zt/U_0 corresponding to the MI-BG and the BG-SF phase transitions. As we have already pointed out earlier that the MI regime corresponds to χ=0, while the BG regime corresponds to $0 < \chi < \chi_c$ till χ_∞=0 and the SF regime is given by, $\chi_c \leq \chi \leq 1$ when $\chi_\infty \neq$0. For that purpose we shall tune zt/U_0 in a controlled manner to closely monitor the value of χ and χ_∞ for a given lattice size namely, L=30. We find that in the antiferromagnetic case (at μ/U_0=0.4), χ is zero till zt/U_0=0.122 at Δ/U_0=0.3, while it is non zero at higher disorder concentration Δ/U_0=0.5. Thus at μ/U_0 =0.4, the onset for the MI-BG transition occurs at zt/U_0=0.122 and the BG phase extends upto zt/U_0=0.133, where χ_c=0.524 with χ_∞=0. Hence the BG-SF transition takes place at zt/U_0=0.133 corresponding to Δ/U_0=0.3. For Δ/U_0=0.5, since there is no MI phase, so the BG-SF phase transition occur at zt/U_0=0.073 with χ_c=0.549.

D. Phase diagram

In this section we will now present the phase diagram of spinor ultracold atoms in $t-\mu$ plane for both the pure and disorder cases based upon the information obtained from ψ_i, χ and χ_∞. In the pure case, the phase diagram can be easily obtained from the information of the SF order parameter, ψ_i, while in the disordered case, we determine our phase diagram depending upon the range of χ as discussed earlier corresponding to both the antiferromagnetic and ferromagnetic cases.

(i) Antiferromagnetic case: In the disorder free case, the phase diagram of spinor ultracold atoms in presence of antiferromagnetic interaction with U_2/U_0=+0.1 is shown in Fig.[8(a)]. It shows that the MI lobes with even occupation densities are somewhat enhanced as compared to the corresponding lobes with odd occupation densities [19, 38]. The MI-SF phase transition for the even MI lobes is first order in nature, while it is second order for the odd MI lobes, as obtained from the variation of the SF order parameter and compressibility which was outlined in the preceding section. The MI phase with even number of bosons per site where each pair of bosons favour the formation of singlet parts and likely are to the more stable and keep themselves isolated from nearest neighbour tunneling. Whereas the MI phase, with odd number of bosons per site, although each pair of bosons can make singlet states, the remaining one is free to tunnel to nearest neighbour sites rendering the odd MI lobes unstable and smaller in width as compared to the even MI lobes.

In presence of disorder, we now try to obtain our phase diagram entirely based on the information obtained from χ. In the previous section, since we distinguished between the three different kind of phases depending upon χ and χ_∞. Thus for obtaining the phase diagram, we set χ=0 as the indicator for the MI phase, $0 < \chi < \chi_c$ (=0.524) for the BG phase and $0.524 \leq \chi \leq 1$ for the SF phase at Δ/U_0=0.3. Similarly for Δ/U_0=0.5, where χ_c is equal to 0.549. The phase diagrams for both the disorder strengths are shown in Figs.[8(b) and 8(c)]. At Δ/U_0=0.3, the intervening BG region for the odd MI lobes is more noticeable as compared to the even MI lobes [see Fig.8(b)]. At Δ/U_0=0.5, the BG phase completely destroys the first odd MI lobe, but the even MI lobe still exists as expected from the earlier discussion [see Fig.8(c)].

(ii) Ferromagnetic case: In Fig.[9(a)], we plot our numerically obtained phase diagram corresponding to the pure case with a ferromagnetic interaction namely,

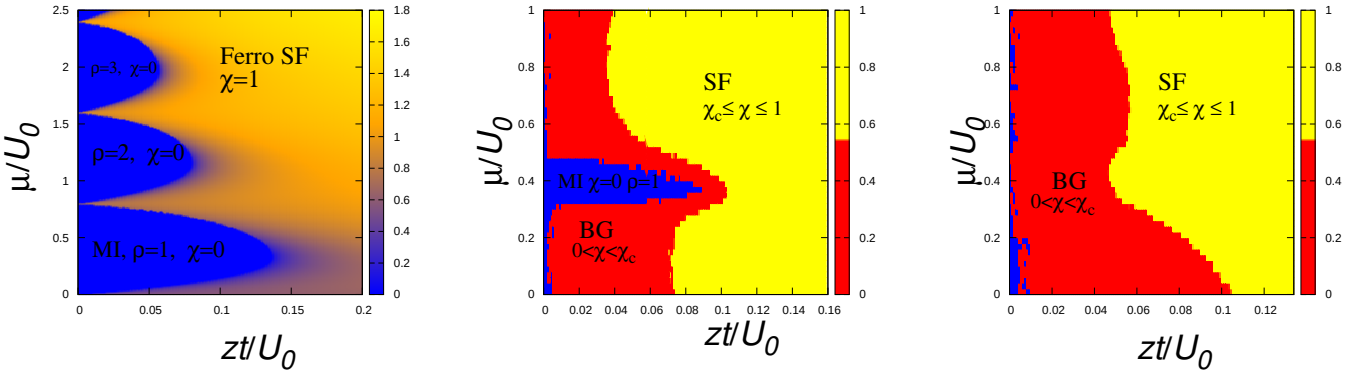

(a) (b) (c)

FIG. 9. (Color online) Phase diagram of spinor ultracold atoms in $t-\mu$ plane at U_2/U_0=-0.2 (ferromagnetic). In the pure case (Δ/U_0=0.0), the phase diagram is similar to that of scalar Bose gas (a). Phase diagram based on the information obtain from χ for the disordered cases, namely Δ/U_0 =0.3 is shown in (b) and Δ/U_0=0.5 in (c).

			Δ/U_0=0	Δ/U_0=0.3		Δ/U_0=0.5	
			MI-SF	MI-BG	BG-SF	MI-BG	BG-SF
Interactions	MI lobes	μ/U_0	zt/U_0	zt/U_0	zt/U_0	zt/U_0	zt/U_0
AF (U_2/U_0=0.1)	first odd	0.4	0.16	0.122	0.133	No	0.073
	first even	1.4	0.26	0.210	0.225	0.123	0.174
F (U_2/U_0=-0.2)	first	0.4	0.133	0.085	0.103	No	0.047

TABLE I. The transition points for the MI-BG and BG-SF phases obtained from χ and χ_∞ for both antiferromagnetic (AF) and ferromagnetic (F) interactions are presented in this table. The corresponding parameter values are mentioned in the table.

U_2/U_0=-0.2. The phases bear similar characteristic features as that of scalar or spinless Bose gas. All the three SF spinor components are non zero in the SF phase which smoothly vary across the MI to SF phases and hence show a second order phase transition. In the disordered case, as earlier, we determine the phase diagram by invoking the critical value of χ_c=0.5034 at Δ/U_0=0.3 and χ_c=0.557 at Δ/U_0=0.5 corresponding to the onset of the SF phase. The phase diagram corresponding to both the disorder values are shown in Figs.[9(b) and 9(c)]. For Δ/U_0=0.5, the MI lobes disappear since the disorder strength is higher than the critical disorder strength and the system is left only with the BG and the SF phases.

IV. CONCLUSIONS

We have studied the effect of onsite disorder in a two dimensional SBHM for both the antiferromagnetic and ferromagnetic interactions. The appearance of the BG phase is observed via the average SF order parameter $\bar{\psi}$ and compressibility $\bar{\kappa}$. The $\bar{\psi}_\sigma$ are zero while $\bar{\kappa}_\sigma$ are zero or constant in MI phase and gradually increases with disorder yielding signature for a BG phase. In the antiferromagnetic case, the MI- SF phase transition for odd MI lobes is always second order while for even MI lobes, it shows second order phase transition with increasing disorder strength. We also find that the MI phase exists till the disorder strength is below the critical value, while it vanishes above the critical value.

Further the three different types of phases, namely the MI, BG and SF phases are identified based on the concept of the SF percolating clusters. We define the MI phase where no SF cluster exists and the SF phase with at least one SF percolating cluster exists. The BG region corresponds in between the MI and SF phase that is the SF cluster exists but does not percolate. We locate the transition point for the MI-BG and the BG-SF phase by calculating the probability of having a percolating cluster χ_∞ (P_{perc}). A percolation analysis of SF percolating cluster is studied using HK algorithm with different system sizes L as a function of tunneling strength, η=zt/U_0 which obey finite size scaling law.

Finally, we obtain our phase diagram based on χ for the antiferromagnetic and ferromagnetic cases. For that purpose, we determine the critical value of χ where a SF clusters percolate first time throughout the lattice and set the respective ranges for χ for three different phases. Thus a reliable enumeration of different phases can be obtained at desired parameter values of the SBHM Hamiltonian. Since these parameters can be precisely controlled in experiments using the properties of the laser fields which superimpose to form optical lattices, our study may have significant impact on the experimental scenario to determine these phases [41].

The transition points for the MI-BG and BG-SF phases obtained from χ and χ_∞ are presented in the table I for

both antiferromagnetic (AF) and ferromagnetic (F) interactions in pure and disordered cases.

Now we shall include some comments concerning the drawbacks in the mean field theory. Since our work is mainly a focus on the effects of disorder in SBHM, thus the single site mean field theory always is not able to handle the site inhomogeneity of the system properly and it works well in higher dimension $d \geq 2$. Although we take into the effect the site inhomogeneity by defining χ, but ignoring quadratic fluctuations introduces a tiny error in the calculations. For example, the MI phase will vanish above the critical disorder strength, our results are in good agreement against this claim within a 3% error.

V. ACKNOWLEDGMENTS

We thank R. V. Pai for useful discussions. SNN likes to thank A. Barman for valuable discussions. SB thanks CSIR, India for financial support under the grants F no: 03(1213)/12/EMR-II.

[1] D.M. Stamper-Kurn, M.R. Andrews, A.P. Chikkatur, S. Inouye, H.-J. Miesner, J. Stenger, and W. Ketterle, Phys. Rev. Lett. **80**, 2027 (1998).
[2] J. Stenger, S. Inouye, D.M. Stamper-Kurn, H.-J. Miesner, A.P. Chikkatur, and W. Ketterle, Nature (London), **396**, 345 (1998).
[3] D.M. Stamper-Kurn, H.J. Miesner, A.P. Chikkatur, S. Inouye, J. Stenger, and W. Ketterle, Phys. Rev. Lett., **83**, 661 (1999).
[4] T.-L. Ho and S.K. Yip, Phys. Rev. Lett., **84**, 4031 (2000).
[5] A. Wagner, C. Bruder, and E. Demler, Phys. Rev. A, **84**, 063636 (2011).
[6] J.-M. Hou and Mo-L. Ge, Phys. Rev. A, **67**, 063607 (2003).
[7] M.D. Barrett, J.A. Sauer, and M.S. Chapman, Phys. Rev. Lett., **87**, 010404 (2001).
[8] M.-S. Chang, C.D. Hamley, M.D. Barrett, J.A. Sauer, K.M. Fortier, W. Zhang, L. You, and M.S. Chapman, Phys. Rev. Lett., **92**, 140403 (2004).
[9] T. Kuwamoto, K. Araki, T. Eno, and T. Hirano, Phys. Rev. A, **69**, 063604 (2004).
[10] H. Schmaljohann, M. Erhard, J. Kronjager, M. Kottke, S. van Staa, L. Cacciapuoti, J.J. Arlt, K. Bongs, and K. Sengstock, Phys. Rev. Lett., **92**, 040402(2004).
[11] D.M. Stamper-Kurn and M. Ueda, Rev. Mod. Phys., **85**, 1191 (2013).
[12] J.E. Lye, L. Fallani, M. Modugno, D. S. Wiersma, C. Fort, and M. Inguscio, Phys. Rev. Lett., **95**, 070401 (2005).
[13] M. White, M. Pasienski, D. McKay, S.Q. Zhou, D. Ceperley, and B. DeMarco, Phys. Rev. Lett., **102**, 055301 (2009)
[14] L. Fallani, J. E. Lye, V. Guarrera, C. Fort, and M. Inguscio , Phys. Rev. Lett., **98**, 130404 (2007).
[15] B. Damski, J. Zakrzewski, L. Santos, P. Zoller, and M. Lewenstein, Phys. Rev. Lett., **91**, 080403 (2003).
[16] A.E. Niederle and H. Rieger, arXiv:1501.03143.
[17] W.S. Bakr, A.Peng, M.E. Tai, R. Ma, J. Simon, J.I. Gillen, S. Flling, L. Pollet, and M. Greiner, Science, **329**, 547 (2010).
[18] J.F. Sherson, C. Weitenberg, M. Endres, M. Cheneau, I. Bloch, and S. Kuhr, Nature, **467**, 68 (2010).
[19] R.V. Pai, K. Sheshadri and R. Pandit, Phys. Rev. B, **77**, 014503 (2008).
[20] S.S. Natu, J.H. Pixley, and S.D. Sarma, Phys. Rev. A, **91**, 043620, (2015).
[21] L. Pollet, N.V. Prokof'ev, B.V. Svistunov, and M. Troyer, Phys. Rev. Lett., **103**, 140402 (2009).
[22] U. Bissbort, R. Thomale, and W. Hofstetter, Phys. Rev. A, **81**, 063643 (2010).
[23] U. Bissbort and W. Hofstetter, Europhys. Lett., **86**, 50007 (2009).
[24] A.E. Neiderle and H. Rieger, New J. Physics, **15**, 075029 (2013).
[25] J.-W. Lee, M.-C. Cha, and D. Kim, Phys. Rev. Lett., **87**, 247006 (2001).
[26] M. Makivic, N. Trivedi, and S. Ullah, Phys. Rev. Lett., **71**, 2307 (1993).
[27] N. Prokofev and B.V. Svistunov, Phys. Rev. Lett., **92**, 015703 (2004).
[28] K. Sheshadri, H.R. Krishnamurthy, R. Pandit, and T.V. Ramakrishnan, Europhys. Lett., **22**, 257 (1993).
[29] A. Barman, S. Dutta, A. Khan, and S. Basu, Eur. Phys. J. B, **63**, 308 (2013).
[30] J. Hoshen, R. Kopelman, Phys. Rev. B, **14**, (1976), 3438.
[31] A. Imambekov, M. Lukin, and E. Demler, Phys. Rev. A, **68**, 063602 (2003).
[32] D.Van Oosten, P.V.D. Straten, and H.T.C. Stoof, Phys. Rev. A, **63**, 053601 (2001).
[33] Tin-Lun Ho, Phys. Rev. Lett., **81**, (1998) 742.
[34] C.K. Law, H. Pu, and N.P. Bigelow, Phys. Rev. Lett., **81**, 5257 (1998).
[35] M. Koashi and M. Ueda, Phys. Rev. Lett., **84**, 1066 (2000).
[36] M.P.A. Fisher, P.B. Weichman, G. Grinstein, and D.S. Fisher, Phys. Rev. B, **40**, 546 (1989).
[37] M. Lacki, S. Paganelli, V. Ahufinger, A. Sanpera, and J. Zakrzewski, Phys. Rev. A, **83**, 013605 (2011).
[38] S. Tsuchiya, S. Kurihara, and T. Kimura, Phys. Rev. A, **70**, 043628 (2004).
[39] T. Kimura, S. Tsuchiya, and S. Kurihara, Phys. Rev. Lett., **94**, 110403 (2005).
[40] D. Stauffer and A. Aharony, *Introduction to Percolation Theory* (Taylor and Francis, 1994)
[41] D. Jaksch, C. Bruder, J.I. Cirac, C.W. Gardiner, and P. Zoller, Phys. Rev. Lett., **81**, 3108 (1998).